Journal of Bioenergetics and Biomembranes (1977) **9**, 223–235

The Relation of Light-Induced Slow Absorbancy and Scattering Changes about 520 nm and Structure of Chloroplast Thylakoids—A Theoretical Investigation

J. T. Duniec and S. W. Thorne[1]

Department of Applied Mathematics, Institute of Advanced Studies, Research School of Physical Sciences, Australian National University, Canberra, A.C.T. 2600, Australia

Received 18 January 1977

Abstract

A theoretical analysis is made on the relation between light-induced thylakoid shrinkage, slow light-induced absorbancy changes about 520 nm, and light-induced scattering changes observed at 90°, which occur in isolated chloroplasts. A simple model of the thylakoids stacks (grana) is assumed and by a mathematical formalism a correlation of these effects is shown. The light minus dark difference spectrum is shown to peak around 520 nm, a fact that confirms earlier suggestions that this difference band is due to the combined effects of the selective dispersion and optical-conformational changes in the grana.

Introduction

When light passes through chloroplasts it is subject to both scattering and absorption. Isolated chloroplasts exhibit reversible light-induced structural changes which may be monitored by electron microscopy, absorbance changes, or 90° light scattering changes [1–6]. Electron microscopy has demonstrated a shrinkage of the thylakoid grana structure upon actinic illumination [4].

[1] Division of Plant Industry, CSIRO, Canberra, 2601, Australia.

Difference spectra (light minus dark) for both absorption and 90° scattering show a peak in the region of 520 nm which cannot be attributed directly to a specific photopigment of the chloroplast. In a recent paper [7] in which both the slow component of the light-induced absorbancy change and the light-induced 90° scattering change were measured and shown to peak in the region of 518 nm, a correlation between the two effects was shown, and it was suggested that the slow absorbancy change was due to the scattering change. It was further concluded that they were both manifestations of the same phenomenon, that of selective dispersion due to light-induced proton uptake with accompanying conformational changes in the chloroplast thylakoid membranes. The peak in the region of 520 nm was suggested to be due to the selective dispersion of the cartenoids but no mathematical appreciation was given.

Changes in light scattering and absorption caused by changes in particle size of biological systems received some theoretical attention earlier [8]. However, selective difference spectra were not discussed, and the origin of the 520 nm peaks remained obscure. To our knowledge, no theoretical investigation has been made to account for this 520 nm band, yet it is important since it is directly linked to the establishment of the high energy state of the energy-transducing photosynthetic mechanism of the chloroplast.

In the present work we give an appreciation of this light-induced phenomenon in terms of optical-conformational changes in the stacked thylakoids (grana) of the chloroplasts. On the basis of a simplified model structure we calculate the effective refractive index of the grana. This is a function of the incident wavelength of the light and the assumed geometrical parameters of the grana stacks. The light-induced hydrogen ion (H^+) uptake by the chloroplast grana is accompanied by an efflux of Mg ions and water which leads to a shrinking or flattening of the thylakoid layers. We assumed that the grana formations of the chloroplasts were sufficiently large to apply the corrected van de Hulst equation [9] to calculate the extinction cross sections in both light and dark conditions. This theoretical approach shows that the model system of grana gives a maximum of the light minus dark difference spectrum in the region of 520 nm. The precise wavelength at which the maximum can occur is model dependent, but lies close to 520 nm for a fairly broad range of parameters.

In the process of the calculation, for simplicity, we have taken account of only two photopigments, chlorophyll a (438, 676) and collectively the carotenoids (500) where the absorbance peaks are given in nanometers. It is known that chlorophyll b is not essential to generate the 520 nm band since a barley mutant without this chlorophyll also gives similar light-induced effects with the same peak [10].

Model and Results

Significant progress has been achieved recently in the study of the structure of chloroplast membranes (thylakoids) and a fluid mosaic membrane model seems plausible [11, 12]. On the basis of this and on recent information concerning chlorophyll–protein complexes, their dimensions, and possible structure [13, 14], we visualize the grana cross sections as shown in Fig. 1. The circles represent the chlorophyll–protein complexes, the sizes of which vary from 80 Å to 160 Å, apparently depending on the type of the complex. These are embedded in the lipid bilayer membrane with possible partial external surface protein layer attached to the intrinsic complexes. These external proteins are not shown in Fig. 1. The fluid cytoplasm is located in the regions between the membranes, and these layers contract upon illumination. The refractive index of cytoplasm may rise slightly due to a loss of water. The effective refractive index of the whole structure changes then for two reasons: (a) a decrease in the volume fraction of cytoplasm in the whole granum and (b) an increase in the refractive index of cytoplasm layers. Changes in scattering and absorbancy of light follow the alterations in the refractive index.

It is well known that multilayered structures are optically anisotropic [15]. This is the reason why we need, in fact, two refractive indices to describe optical properties of grana. Denote by $m^{\perp}$ the refractive index for light polarized perpendicularly to the membranes and by $m^{\parallel}$ the refractive index for light polarized parallel to them. Since the grana absorb light both the refractive indices are complex functions of the wavelength. Let $n^{\perp}$ and $n^{\parallel}$ be the real parts of $m^{\perp}$ and $m^{\parallel}$ respectively, and $-k^{\perp}$ and $-k^{\parallel}$ denote their imaginary parts. In other words, we may express $m^{\parallel}$ and $m^{\perp}$ as follows: $m^{\parallel} = n^{\parallel} - ik^{\parallel}$ and $m^{\perp} = n^{\perp} - ik^{\perp}$. We mention here that in the present case

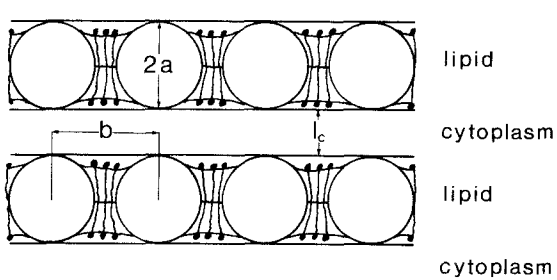

Figure 1. The schematic cross section of grana. The circles represent protein–chlorophyll complexes: a is their radius, b the center-to-center separation. The protein–chlorophyll complexes together with their lipid surround effectively represent a slab of thickness $2a$. The intervening cytoplasmic layers have thickness l_c, and the sandwiched membrane–cytoplasm structure repeats itself many times.

the difference between $m^{\perp}$ and $m^{\parallel}$ is small, thus Figs. 2 and 3 refer to $m^{\perp}$ only; analogical plots for $m^{\parallel}$ would be very similar.

Figure 2 shows the real part of the refractive index of grana–$n^{\perp}(\lambda)$, where λ is the wavelength for light polarized perpendicularly to the membranes. The curve exhibits fluctuations in the values of $n^{\perp}$ around the wavelengths of peak absorptions. This phenomenon is known as selective, or anomalous, dispersion [15, 16]. The calculations leading to Fig. 2 were based on equations derived in the following section. The geometrical parameters used in these are detailed in the caption to Fig. 1. We assumed that chlorophyll a is located solely in the spheres and that the carotenoids were confined to their lipid surround. According to published data [13], the protein-to-chlorophyll ratio in the spheres was taken as 13 : 7; and the carotenoids comprised 4.5% of the remaining lipid mass, i.e., excluding chlorophyll. The absorption bands were centered around 438 nm and 676 nm for chlorophyll a, and 495–500 nm for the carotenoids in vivo.

For the light-induced state the only change made was to reduce the thickness of the cytoplasm layers from 30 Å to 15 Å. The membrane thickness was left unchanged and the volume of a granum stack decreased by 13.6%. In Fig. 3 we plot the light minus dark difference in the refractive index $n^{\perp}$ as a function of wavelength. It is seen from this figure that the increase is not uniform, but fluctuates around the absorption wavelengths in the same manner as does the refractive index (Fig. 2).

For absorbancy calculations a granum structure was assumed to be equivalent to a spherical particle of the mean refractive index $m' = (2m^{\perp} + m^{\parallel})/3$. The particle was immersed in a medium of the refractive index $n_0 = 1.34$, which corresponds to a 0.33 M solution of sorbitol as used in measurements on chloroplasts. Extinction cross sections, which are proportional to measured absorbancies, were calculated for particles having radii of 250, 400, and 500 nm. The extinction cross section is defined as the ratio of the energy of light scattered and absorbed by the particle to the incident energy per unit area [15]. The equivalent spheres were subject to light-induced shrinkage in the same proportion as the grana, i.e., 13.6% in volume. The differences (light minus dark) between the cross sections as functions of wavelength are plotted in Fig. 4. The positions of the maxima depend on the sizes and vary from around 510 nm for the smallest particle to 518 nm for the largest. The curves also show minima around 490 nm.

This explanation of the 520 nm difference band should be treated as a qualitative one. Nevertheless, since we are able to demonstrate this by the application of selective dispersion to a granum model which includes a light-induced shrinkage effect it would seem that the intuitive model is an approach to reality. For simplicity we have assumed that light-induced shrinkage involves only the compression of the intervening cytoplasmic

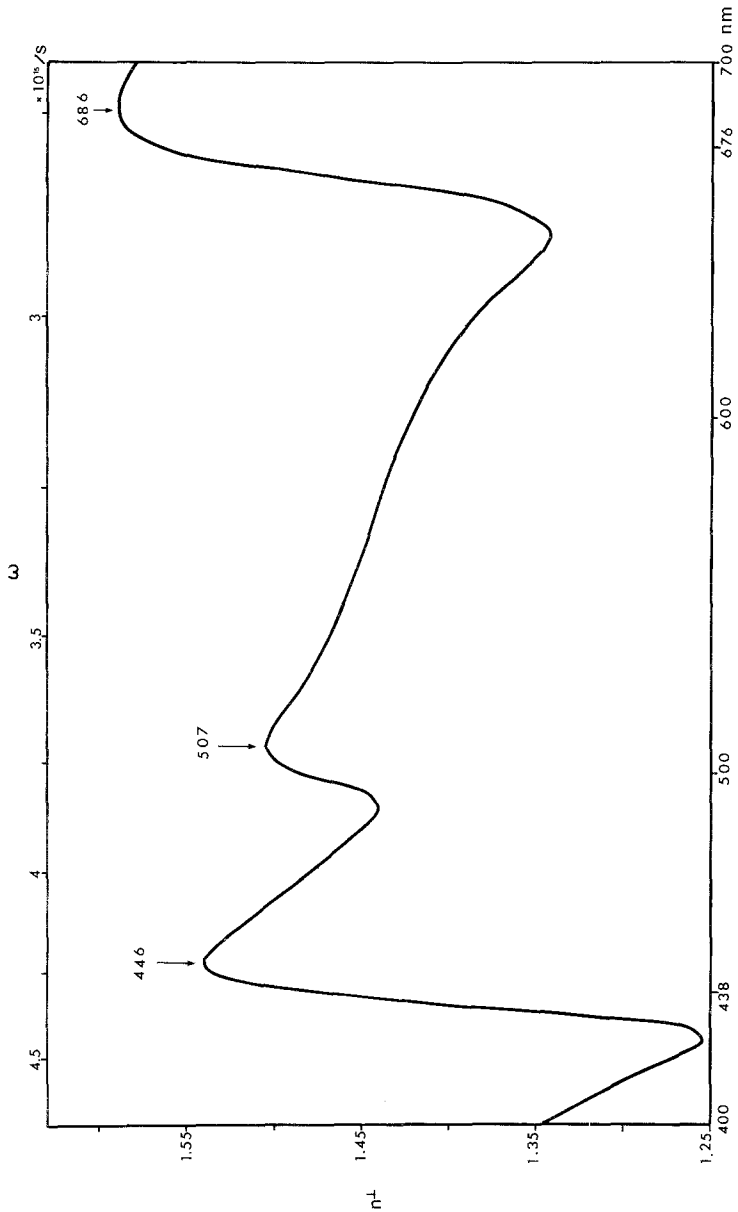

Figure 2. The refractive index of dark adapted grana for light polarized perpendicularly to the membranes versus the wavelength of light.

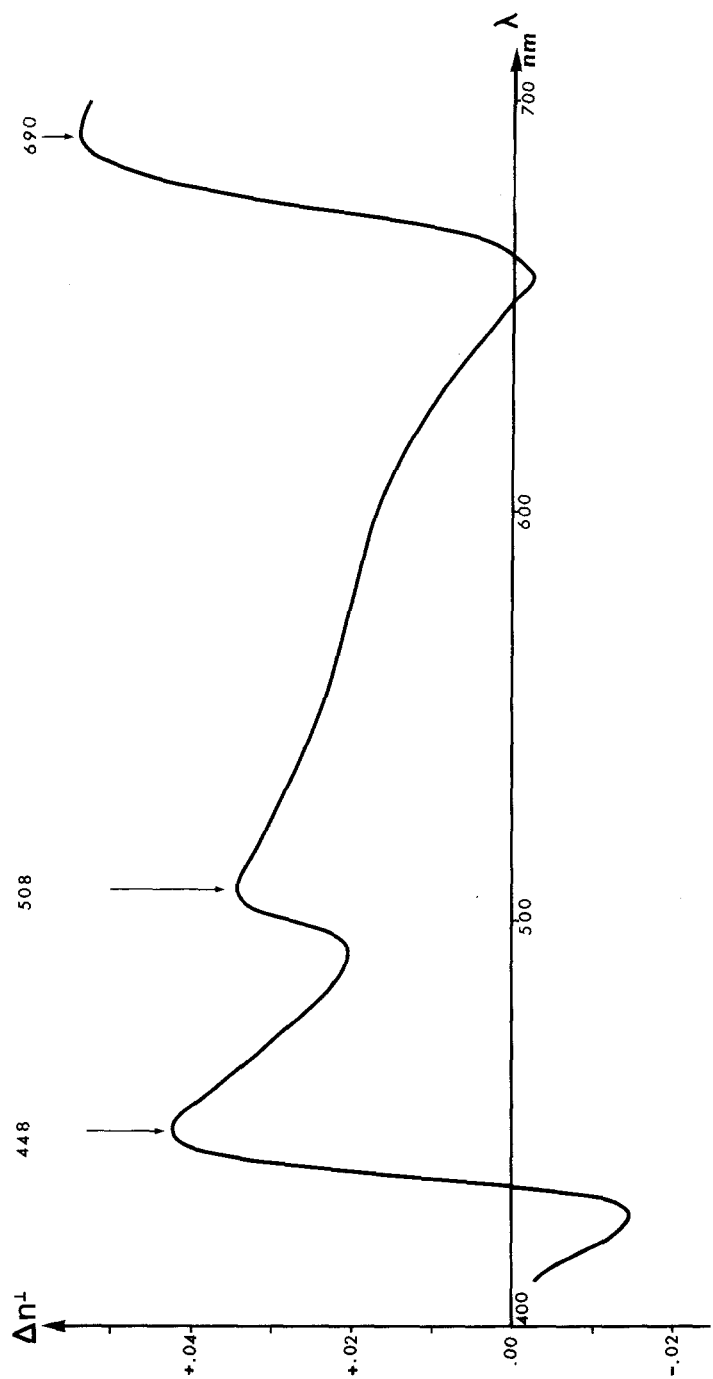

Figure 3. The light minus dark difference in the refractive index $n^{\perp}(\lambda)$ versus the wavelength of light.

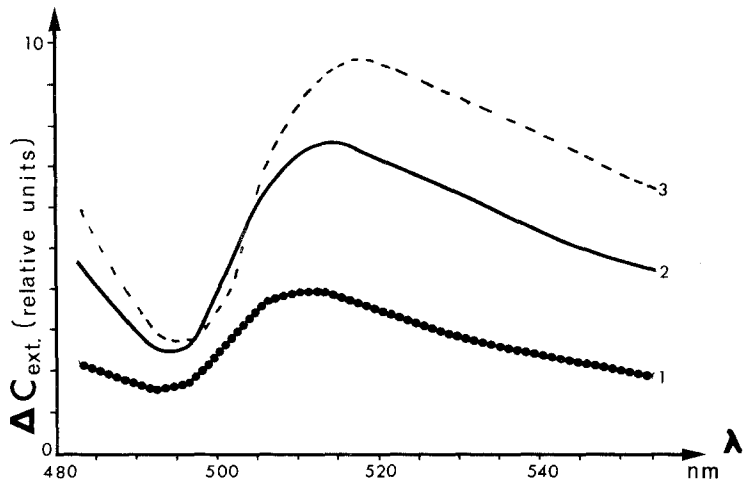

Figure 4. The light minus dark extinction cross sections of spherical particles consisting of grana thylakoids. In the dark the radii of the particles are 250 nm (curve 1), 400 nm (curve 2), and 500 nm (curve 3).

layers; however, in practice the lipid membrane also appears to undergo a light-induced reduction in thickness. This latter change serves only, however, to enhance the nature of the selective dispersion demonstrated, with the maximum optical effects still occurring in the region of 520 nm.

We conclude then that the light-induced shrinkage of the grana structures is indeed responsible for both the slow light-induced absorbancy and 90° light scattering changes which peak in the region of 520 nm. This peak region is determined by the selective dispersion effect associated with the absorbancy bands of the carotenoids and chlorophylls.

Mathematical Details

Several characteristics of light-absorbing materials can be described in terms of the linear damped harmonic oscillator model of the dielectric permittivities [15]. If the material has N absorption frequencies ω_l, $l = 1, 2, \ldots, N$, then its dieletric permittivity can be expressed by an equation

$$\epsilon(\omega) = 1 + \sum_{l=1}^{N} \frac{C_l}{1 - (\omega/\omega_l)^2 - i\gamma_l\omega/\omega_l^2} \tag{1}$$

where the frequency ω is related to the wavelength λ through the relation $\omega = 2\pi c/\lambda$, γ_l are "damping factors" related to the half-widths of the

absorption peaks, and C_l are the absorption strength constants of these. The coefficients C_l can be calculated when the dielectric permittivity is known for frequencies between the absorption bands [17]. In the present case we consider two pigments: chlorophyll and β-carotene. Denote the dielectric permittivities of pure materials by ϵ_{chl} for chlorophyll a and ϵ_{car} for β-carotene. According to Eq. (1), we can write

$$\epsilon_{\text{chl}} = 1 + \frac{C_1}{1-\omega^2/\omega_1^2 - i\gamma_1\omega/\omega_1^2} + \frac{C_2}{1-\omega^2/\omega_2^2 - i\gamma_2\omega/\omega_2^2} + C_3 \tag{2}$$

$$\epsilon_{\text{car}} = 1 + \frac{C_4}{1-\omega^2/\omega_3^2 - i\gamma_3\omega/\omega_3^2} + C_5 \tag{3}$$

Here, ω_1 and ω_2 correspond to the absorption wavelengths of chlorophyll a: 676 and 438 nm, respectively, and ω_3 corresponds to the wavelength of 500 nm taken as the peak absorption for β-carotene in vivo [18]. For the sake of simplicity we considered only one peak of β-carotene, that which is related to the 520 nm difference band. The constants C_3 and C_5 account for contributions from the ultraviolet parts of the spectra; unfortunately, these are not well known, so we make the assumption that these parts of the absorption spectra contribute as much as the visible ones to the dielectric permittivities. For frequencies in the microwave region, when $\omega \ll \omega_1, \omega_2, \omega_3$, the values of ϵ_{chl} and ϵ_{car} should not differ much from the dielectric permittivities of other lipids which may be taken as 2.2. Hence from Eqs. (2) and (3) we obtain, in the low frequency limit,

$$1 + C_1 + C_2 + C_3 \simeq 1 + C_4 + C_5 \simeq 2.2 \tag{4}$$

For simplicity we assume that the extinction coefficients of the 676 and 438 nm absorption peaks are of the same order, and so $C_1 = C_2$; then, keeping in mind the ultraviolet contributions to the permittivities, we obtain

$$C_1 = C_2 = 0.3 \tag{5a}$$

$$C_3 = 0.6 \tag{5b}$$

$$C_4 = C_5 = 0.6 \tag{5c}$$

The constants γ_1, γ_2, and γ_3 are estimated from the half-widths of the absorption peaks; in the calculations the values used are $\gamma_1 = \gamma_2 = 0.14 \times 10^{15}$ sec^{-1}, $\gamma_3 = 0.12 \times 10^{15}$ sec^{-1}.

In the protein–chlorophyll complexes and in the lipid bilayer surrounding them the pigments form only fractions of the total mass. We use the following simple interpolation formulas to express the dielectric constants of the protein–chlorophyll spheres ϵ_s, and their lipid–carotene surround, ϵ_m:

$$\epsilon_s = 1 + v_p(\epsilon_p - 1) + (1 - v_p)(\epsilon_{\text{chl}} - 1) \tag{6}$$

$$\epsilon_m = 1 + v_l(\epsilon_l - 1) + (1 - v_l)(\epsilon_{\text{car}} - 1) \tag{7}$$

where ϵ_p and ϵ_l are the permittivities of nonabsorbing protein and lipid in the visible region, respectively. In the calculations we use the values $v_p = 0.65$ and $v_l = 0.95$, which are simply the corresponding mass fractions of proteins in the spheres and nonabsorbing lipids in the bilayer [13].

The dielectric constant of each cytoplasmic layer between membranes changes as the thickness of each layer decreases, since some water is expelled with an increase in the proportion of suspended protein particles. To account for these changes we use the Lorentz–Lorenz formula [15], which relates the dielectric permittivity of a medium to the polarizability of its molecules. For protein particles suspended in aqueous sucrose of permittivity ϵ_w, the composite dielectric constant ϵ_c can be found from the equation

$$\frac{\epsilon_c - \epsilon_w}{\epsilon_c + 2\epsilon_w} = f\frac{\epsilon_p - \epsilon_w}{\epsilon_p + 2\epsilon_w} \tag{8}$$

where f is the volume fraction of the protein particles in the cytoplasmic layer. It is difficult to estimate this volume fraction, so we fit the value of it which yields $\epsilon_w = (1.35)^2 = 1.82$ in the dark adapted state, given $\epsilon_c = 1.77$ and $\epsilon_p = 2.4$ [19]. When grana are illuminated by light, shrinkage occurs and the volume fraction, f, and ϵ_c both rise. A decrease of thickness by 50%, as we assume in the model calculations, brings about the doubling of the volume fraction and the increase in ϵ_c to 1.90 (refractive index $n_c = 1.38$).

Finally, we proceed to calculate the dielectric permittivity of whole grana. We apply formulae derived in relation to a birefringence problem in vision research by Ninham and Sammut [19]. From these formulas we can calculate the dielectric constant of the structure shown in Fig. 1; given the permittivities of the components: ϵ_s for the spheres, ϵ_m for their lipid surround, and ϵ_c for the composite cytoplasmic layers. First, the dielectric properties of a plane of spheres of radius a, center-to-center separation b, are equivalent to those of an anisotropic dielectric slab of thickness $2a$ and permittivities

$$\epsilon_{\text{pl}}^{\perp} = \epsilon_m \left(\frac{\Delta_{ms} - 9.0338(a/b)^3}{\Delta_{ms} - 9.0338(a/b)^3 + 2\pi a^2/b^2} \right) \tag{9}$$

$$\epsilon_{\text{pl}}^{\parallel} = \epsilon_m \left(\frac{\Delta_{ms} + 4.5169(a/b)^3 - 2\pi a^2/b^2}{\Delta_{ms} + 4.5169(a/b)^3} \right) \tag{10}$$

in the directions perpendicular and parallel to the plane, respectively. The

quantity Δ_{ms} is defined by

$$\Delta_{ms} = \frac{2\epsilon_m + \epsilon_s}{\epsilon_m - \epsilon_s} \tag{11}$$

Second, the medium consisting of stacks of these slabs, separated by intervening cytoplasmic layers of dielectric permittivity ϵ_c and thickness l_c (see Fig. 1), has the permittivities [15, 19]

$$\epsilon^{\perp} = (l_c + 2a)\left(\frac{l_c}{\epsilon_c} + \frac{2a}{\epsilon^{\perp}_{pl}}\right) \tag{12}$$

$$\epsilon^{\parallel} = \frac{l_c\epsilon_c + 2a\epsilon^{\parallel}_{pl}}{l_c + 2a} \tag{13}$$

Note that Eqs. (12) and (13) are valid even when the thickness of the layers varies, provided the overall structure is periodic and the spatial period is small compared with the wavelength of light. In such a case, l_c should be replaced by the mean over the period.

Now, the refractive indices of grana for light polarized parallel to the membranes, $m^{\parallel}$, and for light polarized perpendicularly to them, $m^{\perp}$, are readily obtained from Eqs. (12) and (13) by applying the familiar Maxwell's relations:

$$(m^{\parallel})^2 = \epsilon^{\parallel} \tag{14a}$$

$$(m^{\perp})^2 = \epsilon^{\perp} \tag{14b}$$

Equations (14a) and (14b) conclude the calculation of the refractive indices of grana. Both $m^{\parallel}$ and $m^{\perp}$ are complex since the permittivities ϵ_m and ϵ_s are. The light-induced changes in grana structures are reflected in changes in the values of $m^{\parallel}$ and $m^{\perp}$ since (a) the thickness l_c is decreased [cf. Eqs. (12) and (13)] and (b) the value of ϵ_c is changed with the increase in the fraction of protein particles suspended in the cytoplasm [Eq. (8)].

In order to calculate the light-induced absorbancy changes we identify a granum structure of chloroplasts with an equivalent spherical particle of radius R and mean refractive index $m' = (m^{\parallel} + 2m^{\perp})/3$. The particle is assumed to be in a medium of the refractive index $n_0 = 1.34$. Denote by m the relative refractive index of the particle: $m = m'/n_0$. Denote also the real part of m by n and the imaginary part by $-k$, so that $m = n - ik$. We apply the van de Hulst equation of anomalous diffraction [9, 20] to calculate the extinction efficiency of the particle, Q_{ext}:

$$Q_{ext} = 2 - 4\exp(-\rho\tan\beta)\left(\cos\frac{\beta}{\rho}\right)\sin(\rho-\beta) - 4\exp(-\rho\tan\beta)\left[\frac{(\cos\beta)^2}{\rho^2}\right]\cos(\rho-2\beta) + 4\left(\cos\frac{\beta}{\rho}\right)^2\cos 2\beta \tag{15}$$

where $\rho = 4\pi R(n-1)/\lambda$ and $\tan\beta = k/(n-1)$. The extinction efficiency is defined as the energy of light scattered and absorbed by the particle to the incident energy geometrically intercepted by the particle; the extinction cross section, C_{ext}, is related to Q_{ext} by the formula

$$C_{ext} = \pi R^2 Q_{ext} \tag{16}$$

Equation (15) applies only to particles larger than the wavelength of light. However, there are empirical corrections derived by Deirmendjian [21, 20], which bring the values of Q_{ext} to within ±4% of the exact ones calculated from Mie's theory. The corrected value of the extinction efficiency is

$$Q'_{ext} = (1 + D_i)Q_{ext} \tag{17}$$

where Q_{ext} is given by Eq. (15) and the factors D_i are specified for four ranges of ρ provided that $1 \leqslant n \leqslant 1.50$ and $0 \leqslant k \leqslant 0.25$:

$$D_1 = 0.61(n-1)^2\,\frac{F(\beta)+1}{n} - \frac{5(n-1)-\rho}{5(n-1)F(\beta)} \tag{18}$$

for $\rho \leqslant 5(n-1) < 4.08/(1+3\tan\beta)$;

$$D_2 = 0.123(n-1)\,\frac{[F(\beta)+1]\rho}{n} \tag{19}$$

for $5(n-1) \leqslant \rho \leqslant 4.08/(1+3\tan\beta)$;

$$D_3 = 0.5(n-1)\,\frac{F(\beta)+1}{n(1+3\tan\beta)} \tag{20}$$

for $4.08/(1+3\tan\beta) \leqslant \rho \leqslant 4.08/(1+\tan\beta)$;

$$D_4 = 2.04(n-1)\,\frac{F(\beta)+1}{n\rho F(\beta)} \tag{21}$$

for $\rho > 4.08/(1+\tan\beta)$. In these equations $F(\beta)$ is defined by

$$F(\beta) = (1+\tan\beta)(1+3\tan\beta) \tag{22}$$

The calculations which serve to plot Fig. 4 are performed for three particles having radii of 250, 400, and 500 nm. Upon illumination they are taken to shrink to 216, 345.6, and 432 nm, respectively. Their refractive

index, m, changes in the way described earlier. The absorbancy changes are proportional to the changes in the extinction cross sections, since the absorbancy, E, is related to C_{ext} by the equation [8]

$$E = 0.434LNC_{ext} \tag{23}$$

where $E = \log_{10}(1/\text{transmission})$, L is the vessel thickness, and N is the concentration of particles.

To conclude this section it seems worthwhile to discuss to what degree the measured scattering and absorbancy changes are due to the grana formations. Apart from the grana, light is also scattered and absorbed at stroma membranes and chloroplast envelopes. However, as the measurements of Krause [22] show, for chloroplast suspensions in which grana are artificially unstacked the absorbancy and scattering are significantly lower compared with intact chloroplasts. Thus the absorbancy and scattering changes must be due predominantly to the changes within the grana. This also supports the view that the development of grana is necessary to achieve increased absorbancy of light by chloroplasts.

Acknowledgments

The authors are grateful to Dr. Jan M. Anderson for a helpful discussion and Professor B. W. Ninham for his interest and encouragement.

References

1. L. Packer, *Biochem. Biophys. Res. Commun.*, **9** (1962) 355.
2. M. Itoh, S. Izawa, and K. Shibata, *Biochim. Biophys. Acta,* **66** (1963) 319.
3. L. Packer and D. W. Deamer, in: *Photophysiology,* A. C. Giese (Ed.), Academic Press, New York, Vol. 3 (1964), p. 91.
4. S. Murakami and L. Packer, *J. Cell Biol.,* **47** (1970) 322.
5. L. Packer and P. A. Sigenthaler, *Int. Rev. Cytol.,* **20** (1966) 97.
6. A. R. Crofts, D. W. Deamer, and L. Packer, *Biochim. Biophys. Acta,* **131** (1967) 97.
7. S. W. Thorne, G. Horvath, A. Kahn, and N. K. Boardman, *Proc. Natl. Acad. Sci. U.S.A.,* **72** (1975) 3858.
8. P. Latimer, D. M. Moore, and F. D. Bryant, *J. Theor. Biol.,* **21** (1968) 348.
9. H. C. van de Hulst, *Light Scattering by Small Particles,* Wiley, New York (1957).
10. S. W. Thorne and N. K. Boardman, unpublished results.
11. F. S. Sjöstrand and L. Barajas, *J. Ultrastruct. Res.,* **32** (1970) 293.
12. S. J. Singer and G. L. Nicholson, *Science,* **175** (1972) 720.
13. J. M. Anderson, *Biochim. Biophys. Acta,* **416** (1975) 191.
14. J. M. Anderson, *Nature (London),* **253** (1975) 536.
15. M. Born and E. Wolf, *Principles of Optics,* 3rd ed., Pergamon, Oxford (1965).
16. P. Latimer and E. Rabinowitch, *Arch. Biochem. Biophys.,* **84** (1959) 428.
17. D. Gingell and V. A. Parsegian, *J. Theor. Biol.,* **36** (1972) 41.
18. E. Rabinowitch and Govindjee, *Photosynthesis,* Wiley, New York (1969).
19. B. W. Ninham and R. A. Sammut, *J. Theor. Biol.,* **56** (1976) 125.

20. M. Kerker, *The Scattering of Light and Other Electromagnetic Radiation,* Academic Press, New York (1969).
21. D. Deirmendjian, *Q. J. Roy. Meteorol. Soc.,* **86** (1960) 371.
22. G. H. Krause, in: *Proceedings 3rd International Congress on Photosynthesis, September 2–6, 1974, Rehovot, Israel,* Elsevier, Amsterdam (1974).